

Experimental Determination of Reorientational Correlation Time of CO₂ over a Wide Range of Density and Temperature

Tatsuya Umecky,^{*,†,‡} Mitsuhiro Kanakubo,^{*,†} and Yutaka Ikushima[†]

Supercritical Fluid Research Center, National Institute of Advanced Industrial Science and Technology (AIST), Nigatake 4-2-1, Miyagino-ku, Sendai 983-8551, Japan, CREST, Japan Science and Technology Corporation (JST), Honcho 4-1-8, Kawaguchi, Saitama 332-0012, Japan, and Department of Chemistry, Graduate School of Science, Tohoku University, Aramaki, Aoba-ku, Sendai 980-8578, Japan

Received: December 16, 2002; In Final Form: June 9, 2003

We have precisely measured ¹⁷O longitudinal relaxation times, $T_1(^{17}\text{O})$, of CO₂ under gaseous, liquid, and supercritical conditions at four different temperatures of 293.4, 313.0, 331.8, and 351.4 K over a wide pressure range between 1 and 20 MPa, corresponding to a density range between 0.03 and 0.94 g cm⁻³. Assuming that the quadrupolar interaction is a dominant mechanism in the ¹⁷O relaxation, the reorientational correlation time, τ_{2r} , of CO₂ was obtained from $T_1(^{17}\text{O})$ with a known value of the quadrupole coupling constant. The τ_{2r} in CO₂ thus determined showed a unique density dependence; τ_{2r} decreased rapidly with increasing density at lower densities up to ~ 0.2 g cm⁻³, τ_{2r} seemed to be insensitive at intermediate densities between 0.2 and 0.6 g cm⁻³, and τ_{2r} moderately increased at higher densities more than 0.6 g cm⁻³. It was demonstrated that the density dependence of τ_{2r} in CO₂ has a clear minimum near the critical density. The present experimental results of τ_{2r} perfectly agreed with the calculation ones recently reported by Adams and Siavosh-Haghighi (*J. Phys. Chem. B* 2002, 106, 7973). The rotational dynamics of CO₂ was discussed over a wide range of density and temperature in terms of τ_{2r} together with the angular momentum correlation time.

1. Introduction

Supercritical fluids have an advantage over conventional liquid solvents; i.e., its solvent properties such as a dielectric constant, solubility parameter, and diffusivity can be tuned widely and successively by adjusting temperature and pressure. In particular, because carbon dioxide is nonflammable, nontoxic, and inexpensive and its critical point ($T_c = 304.2$ K, $p_c = 7.38$ MPa, and $\rho_c = 0.466$ g cm⁻³)¹ is relatively moderate, supercritical CO₂ is expected to be one of the most desirable environmentally benign media for an extraction, separation, and reaction processes.² To promote such application of supercritical CO₂, it is of great importance to derive the optimum conditions after understanding the solvent properties sufficiently. In the present study, hence, we will offer one of the most fundamental quantities of the reorientational correlation time in pure CO₂ over a wide range of density and temperature on the basis of experimental results. Because the rotational dynamics of a CO₂ molecule solvated around a solute or reaction species will be a little different from that in the pure solvent, the reorientational correlation time determined can be evaluated to be the characteristic parameter of solvation dynamics in terms of the reorientational process in sub- and supercritical CO₂ solutions.³

A rotational motion of a molecule sensitively reflects the local solvent environment because it is perturbed by an effective friction arising from intermolecular interactions between the rotating and surrounding molecules. There will be, at least, two extreme situations considered in the rotational process. One is often called the Debye diffusion model,⁴ describing the molec-

ular reorientation as a small step angular random walk. The other may be what is called the inertial rotation or the free-rotor, where the molecule can rotate freely during a period perturbed by molecular collisions. Thus, the former situation frequently applies to a "liquid-like" dense fluid, whereas the latter refers to a "gas-like" sparse fluid. Supercritical CO₂ can provide an opportunity to investigate the rotational dynamics over an entire range of density from the liquidlike to gaslike through intermediate without a phase separation.

To estimate the rotation dynamics of a molecule quantitatively, a reorientational correlation function, $C_{lr}(t)$, and/or its time-integral of a reorientational correlation time, τ_{lr} , has frequently been used:

$$\tau_{lr} = \int_0^\infty C_{lr}(t) dt \quad (1)$$

where the subscript "l" indicates the order of the Legendre polynomial. These quantities can be determined by molecular dynamics simulation as well as various experimental techniques such as infrared absorption, dielectric relaxation, Rayleigh, Raman scattering, fluorescence, and NMR relaxation measurements.⁵ And also, time-resolved spectroscopy gives the time-dependent reorientational correlation function.⁶ NMR relaxation measurements used in this study have widely been applied to a variety of systems⁷ because many kinds of NMR active nuclei are available for both organic and inorganic compounds. An NMR longitudinal relaxation time, T_1 , can be related to the second-order reorientational correlation time, τ_{2r} , in many cases, although the time-dependent reorientational correlation function cannot be obtained. Moreover, a suitable choice of nucleus in a molecule can provide meaningful information about the angular momentum correlation time, τ_J , as well as τ_{2r} . This is the case for the present target of a CO₂ molecule despite its

* To whom correspondence should be addressed. Tel: +81-22-237-5211. Fax: +81-22-237-5224. E-mail: t-umecky@aist.go.jp; m-kanakubo@aist.go.jp.

[†] Supercritical Fluid Research Center and CREST.

[‡] Tohoku University.

simple structure with only two kinds of NMR active nuclei, ^{17}O and ^{13}C . The former quadrupolar ^{17}O with the spin quantum number, I , being $5/2$, can relax through the intramolecular interaction between the nuclear quadrupole moment and the electric field gradient at the nucleus. Thus, the ^{17}O longitudinal relaxation time, $T_1(^{17}\text{O})$, in CO_2 can be inversely related to τ_{2r} under the extreme narrowing condition:⁸

$$\frac{1}{T_1(^{17}\text{O})} = \frac{3\pi^2}{10} \frac{2I+3}{I^2(2I-1)} \left(1 + \frac{\eta_q^2}{3}\right) \left(\frac{eQq}{h}\right)^2 \tau_{2r} \quad (2)$$

where eQq/h is the quadrupole coupling constant and η_q is the asymmetry parameter. On the other hand, because a CO_2 molecule has little nuclei with magnetic moments in natural abundance, the ^{13}C longitudinal relaxation time, $T_1(^{13}\text{C})$, in CO_2 can be predominantly determined by the spin-rotation mechanism over a wide range of density and temperature.^{9–11} Hence, $T_1(^{13}\text{C})$ for a linear CO_2 molecule can be given by the following equation under the extreme narrowing condition:⁸

$$\frac{1}{T_1(^{13}\text{C})} = \frac{16\pi^2 C_\perp^2 I k_B T}{3h^2} \tau_J \quad (3)$$

where C_\perp is the spin-rotation coupling constant and I is the momentum of inertia. By reason of much higher sensitivity of ^{13}C than ^{17}O , several researchers^{9–11} have already determined τ_J of CO_2 from $T_1(^{13}\text{C})$.

In the last one or two decades, there have been some dozen studies^{12–25} to discuss quantitatively the rotational dynamics of solute molecules in binary solutions of supercritical CO_2 in terms of solute–solvent interactions. As yet, however, there have been only a few reports on the rotational dynamics in neat CO_2 . In 1981, Versmold²⁶ reported the reorientational correlation functions, $C_{2r}(t)$, of CO_2 at six densities from 0.05 and 1.1 g cm^{-3} at a fixed temperature of 313 K by depolarized Rayleigh scattering measurements. At lower densities, $C_{2r}(t)$ never asymptotically decayed to zero and the temporal behavior of $C_{2r}(t)$ was described by the J -diffusion model almost perfectly. At higher densities, in contrast, the simple exponential decay of $C_{2r}(t)$ was observed except for the very short time range. Recently, Holz et al.²⁷ determined τ_{2r} of CO_2 over a density range from 0.19 to 1.0 g cm^{-3} at two temperatures of 298 and 319 K by ^{17}O NMR relaxation measurements. The Debye–Einstein–Stokes and J -diffusion models gave only a qualitative description of τ_{2r} in limited density ranges. Using molecular dynamics simulation, more recently, Adams and Siavosh-Haghighi²⁸ computed not only the time-dependent first and second reorientational correlation functions but also the time-dependent angular velocity correlation function together with their integral correlation times in CO_2 over a density range from 0.05 to 1.0 g cm^{-3} at a fixed temperature of 307 K 1% above the critical temperature. They confirmed that the calculated results were not far from the experimental ones of Versmold²⁶ and Holz et al.,²⁷ and concluded that the reorientational correlations may be characterized as the “diffusive”, i.e., the Debye diffusion model, only at densities in excess of the critical density. The noteworthy simulation study of Adams and Siavosh-Haghighi²⁸ can shed a bright light on the density dependence of the rotational dynamics in CO_2 , and consequently, it has highlighted much more importance and necessity of the reliable experimental data over a wide experimental condition. In this study, hence, with our developed in situ NMR observation technique,^{24,29,30} we experimentally determine τ_{2r} in CO_2 from $T_1(^{17}\text{O})$ over a wide range of density and temperature.

2. Experimental Section

To accurately determine NMR relaxation times of less sensitive ^{17}O in CO_2 , we have improved the previous high-pressure cell, which was made of easy-machinable poly(ether ether ketone).^{24,30,31} A 5.2 mm inner diameter in the high-pressure cell with 10 mm outer diameter was carefully enlarged to be 6.2 mm. As a result, the sample volume was increased approximately 1.5 times, which can result in a rise in signal-to-noise ratio almost in proportion. Although the pressure tolerance was devalued, the improved cell adequately withstood temperature and pressure, at least, up to 373 K and 35 MPa, respectively. We have confirmed no background noise in ^{17}O spectra as well as ^1H and ^{13}C spectra. Minor modifications in the high-pressure cell were made for the simple handling and safety consideration (see the Supporting Information). The present high-pressure polymer cell had a higher filling factor of ~ 1.5 times or more than the glass cell previously used by Holz et al.²⁷ This can provide the precise relaxation data even under very dilute conditions at low densities.

The improved high-pressure cell was connected to a syringe pump (Isco, 260D) and pressure gauge (Druck, DPI145) and then was installed in an NMR probe, where the schematic diagram of high-pressure NMR setup was given in the Supporting Information. After completely replacing the air containing paramagnetic oxygen in the high-pressure system, a sample of CO_2 (Showa Tansan Co., Ltd., 99.99 vol % up) was introduced into the high-pressure cell at a desired pressure with the syringe pump. The sample temperature was controlled by a heated dry gas with a variable temperature control unit equipped with a spectrometer and was calibrated with a calibrated thermistor thermometer (Takara, D641). The sample pressure was recorded as the absolute pressure. The temperature and pressure fluctuations during each measurement were within ± 0.1 K and ± 0.1 MPa, respectively, over the observed range.

^{17}O NMR spectra were obtained using a Varian Inova 500 spectrometer equipped with a standard 10 mm probe, where the resonance frequency was 67.77 MHz. The free induction decays were accumulated 16–2048 times, and the signal-to-noise ratios were confirmed to be more than ~ 25 under a thermally equilibrium condition. The ^{17}O signals of CO_2 were observed clearly enough to determine T_1 (see the Supporting Information). The ^{17}O longitudinal relaxation times, $T_1(^{17}\text{O})$, of CO_2 were measured at 293.4, 313.0, 331.8, and 351.4 K over a pressure range from 1 to 20 MPa with a standard inversion–recovery pulse sequence (PD– π – t – $\pi/2$ –detect), where PD was the fixed pulse delay longer than $5T_1$ and t was the variable time. In each measurement, a set of more than 15 different values was used for t . We have repeatedly determined $T_1(^{17}\text{O})$ five times or more under each condition. They were reproducible within a few percent of errors independent of CO_2 density. Before each run of $T_1(^{17}\text{O})$ measurements, ^{13}C relaxation times, $T_1(^{13}\text{C})$, of CO_2 were measured at higher pressures of ~ 20 MPa and were compared with the literature values.^{9,10} Because a small amount of paramagnetic oxygen appreciably shortens $T_1(^{13}\text{C})$ of CO_2 at such higher pressures, a good agreement of our $T_1(^{13}\text{C})$ with the literature values showed no contamination of air containing oxygen in the prepared samples.

3. Results and Discussion

^{17}O NMR longitudinal relaxation times, $T_1(^{17}\text{O})$, of CO_2 were measured on four isotherms of 293.4, 313.0, 331.8, and 351.4 K at pressures from 1 to 20 MPa, corresponding to at densities from 0.03 to 0.94 g cm^{-3} (Table 1). The density dependence of $T_1(^{17}\text{O})$ is given in Figure 1 (please see the left-hand axis). The

TABLE 1: $T_1(^{17}\text{O})$ of CO₂ at Four Different Temperatures over a Wide Density Range^a

293.4 K			313.0 K			331.8 K			351.4 K		
p/MPa	$\rho/\text{g cm}^{-3}$	T_1/s	p/MPa	$\rho/\text{g cm}^{-3}$	T_1/s	p/MPa	$\rho/\text{g cm}^{-3}$	T_1/s	p/MPa	$\rho/\text{g cm}^{-3}$	T_1/s
1.4	0.027	0.045 (4)	2.3	0.043	0.072 (11)	2.3	0.041	0.064 (2)	2.3	0.037	0.060 (8)
2.4	0.050	0.081 (4)	3.2	0.064	0.104 (7)	3.3	0.060	0.094 (6)	3.3	0.055	0.092 (3)
3.4	0.078	0.127 (5)	4.2	0.089	0.131 (6)	4.2	0.080	0.125 (2)	4.2	0.072	0.113 (4)
4.3	0.108	0.164 (3)	5.1	0.118	0.173 (5)	5.0	0.100	0.155 (7)	5.3	0.096	0.145 (5)
5.1	0.148	0.197 (3)	6.4	0.165	0.218 (7)	6.4	0.138	0.193 (5)	6.4	0.122	0.178 (10)
6.5	0.794	0.218 (1)	7.1	0.204	0.234 (9)	7.4	0.170	0.213 (7)	7.3	0.144	0.198 (11)
8.4	0.832	0.211 (1)	8.0	0.285	0.254 (7)	8.2	0.203	0.237 (9)	8.2	0.169	0.216 (6)
10.0	0.854	0.208 (3)	8.7	0.402	0.262 (7)	9.2	0.250	0.254 (6)	9.2	0.199	0.237 (14)
12.5	0.882	0.203 (2)	9.2	0.535	0.259 (4)	10.4	0.324	0.269 (6)	10.2	0.231	0.251 (5)
14.0	0.895	0.201 (1)	9.6	0.592	0.256 (3)	11.2	0.384	0.276 (2)	10.9	0.260	0.266 (9)
16.0	0.911	0.199 (2)	10.6	0.670	0.248 (2)	12.2	0.469	0.273 (5)	12.3	0.316	0.274 (3)
18.0	0.924	0.196 (1)	12.4	0.732	0.241 (4)	13.2	0.537	0.273 (6)	13.1	0.354	0.280 (7)
20.8	0.941	0.194 (1)	13.9	0.765	0.237 (4)	14.3	0.591	0.269 (5)	14.1	0.400	0.284 (5)
			16.1	0.798	0.231 (2)	15.9	0.649	0.266 (5)	16.2	0.491	0.285 (5)
			17.7	0.818	0.229 (2)	18.0	0.697	0.261 (3)	18.4	0.565	0.282 (4)
			20.5	0.846	0.226 (2)	20.3	0.737	0.255 (5)	20.5	0.618	0.281 (4)

^a The 95% confidence limit in the least significant digits is given in parentheses.

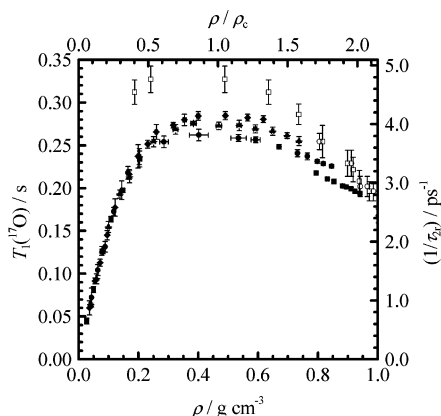


Figure 1. Density dependence of $T_1(^{17}\text{O})$ (left-hand axis) and $1/\tau_{2r}$ (right-hand axis) of CO₂ at 293.4 (■), 313.0 (●), 331.8 (▲), and 351.4 K (◆). The previously reported values²⁷ were represented by the open symbols at 298 (□) and 319 (○) K.

vertical error bars represent the 95% confidence limits of $T_1(^{17}\text{O})$ obtained by five or more repeated runs and the horizontal error bars indicate the maximum uncertainties in CO₂ density calculated from the temperature and pressure fluctuations. As described in the Introduction, $T_1(^{17}\text{O})$ of quadrupolar ^{17}O can give the second-order reorientational correlation time, τ_{2r} , of CO₂ in terms of the O=C=O bond axis if the values of eQq/h and η_q are known. eQq/h of ^{17}O in gaseous CO₂ was experimentally determined to be -3.92 MHz by microwave spectroscopy.³² Holz et al.,²⁷ moreover, have recently confirmed that eQq/h in CO₂ remains constant and η_q is negligible over a wide range of temperature (298–325 K) and density (0.004 – 1.0 g cm⁻³) using a combination of molecular dynamics and quantum chemical simulations. Hence, we obtain τ_{2r} of CO₂ from $T_1(^{17}\text{O})$ by substituting $eQq/h = -3.92$ MHz and $\eta_q = 0$ into eq 2. The density dependence of $1/\tau_{2r}$ is also shown in Figure 1 (right-hand axis) together with the values previously reported by Holz et al.²⁷ Our $1/\tau_{2r}$ values appear to be smaller than Holz's ones at densities up to ~ 0.8 g cm⁻³, whereas the two data agree with each other within the experimental errors at higher densities. As seen from Figure 1, the uncertainties in $1/\tau_{2r}$ were much improved in the present experiments. This may be primarily attributable to an increase in the signal-to-noise ratios in ^{17}O spectra due to the modification of the high-pressure cell. The improvement newly reveals that $1/\tau_{2r}$ is slightly dependent on temperature at high densities. Moreover, the

TABLE 2: Values of σ_{2r} in CO₂ at Four Different Temperatures^a

	293.4 K	313.0 K	331.8 K	351.4 K
$(\partial\tau_{2r}^{-1}/\partial\rho)/10^{-15} \text{ m}^3 \text{ s}^{-1}$	1.66 (4)	1.65 (6)	1.65 (1)	1.66 (3)
$\sigma_{2r}/10^{-20} \text{ m}^2$	313 (7)	300 (10)	292 (2)	286 (6)

^a The 95% confidence limit in the least significant digits is given in parentheses. ^b $\partial\tau_{2r}^{-1}/\partial\rho$ was determined at low densities up to ~ 0.1 g cm⁻³.

present experimental data over a wide density range can provide a consistent picture of molecular reorientation from the gaslike to liquidlike through “intermediate” states. In the gaslike state up to $\rho \approx 0.2$ g cm⁻³ $1/\tau_{2r}$ of CO₂ rapidly increases with increasing density almost in proportion, in the intermediate state at $\rho \approx 0.2$ – 0.6 g cm⁻³ $1/\tau_{2r}$ appears to be insensitive to density, and in the liquidlike state at $\rho > 0.6$ g cm⁻³ $1/\tau_{2r}$ moderately decreases with increasing density.

In the gaslike state up to $\rho \approx 0.2$ g cm⁻³, it was observed that $1/\tau_{2r}$ is proportional to density. This density dependence is attributable to the fact that the temporal behavior of $C_{2r}(t)$ at such lower densities does not follow a simple exponential decay but a oscillatory decay as observed by Rayleigh scattering²⁶ and computed by molecular dynamics simulation.²⁸ Accordingly, as ρ decreases, i.e., the rotating molecules lose their correlations, $C_{2r}(t)$ should approach the corresponding profile in the free-rotor. Therefore, its integral of τ_{2r} increases and will diverge infinitely as ρ decreases to zero. Jameson et al.^{33,34} have empirically analyzed the density dependence of $1/\tau_{2r}$ in terms of molecular collision on the basis of the gas kinetic theory:

$$\frac{1}{\tau_{2r}} = \rho_N \sigma_{2r} \bar{v} \quad (4)$$

where ρ_N is the number density, σ_{2r} is the effective collision cross section, and \bar{v} is the mean relative velocity ($=\sqrt{8k_B T/\pi\mu}$, where μ is the reduced mass). From a linear density dependence of quadrupolar ^{14}N relaxation time in N₂ gas, Jameson et al.³⁴ presented $\sigma_{2r}(\text{N}_2) = 29.6 \times 10^{-20} \text{ m}^2$ at 300 K and $\sigma_{2r}(\text{N}_2) \propto T^{-0.67 \pm 0.02}$. In a similar manner, we can obtain σ_{2r} for CO₂ at each temperature by linearly fitting the experimental data in the range of $\rho < 0.1$ g cm⁻³ (Table 2). This leads to $\sigma_{2r}(\text{CO}_2) = 308 \times 10^{-20} \text{ m}^2$ at 300 K and $\sigma_{2r}(\text{CO}_2) \propto T^{-0.50 \pm 0.04}$. $\sigma_{2r}(\text{CO}_2)$ is larger than $\sigma_{2r}(\text{N}_2)$ by a factor of ~ 10 . If one takes into account the geometric cross sections of $\sigma_{\text{geom}}(\text{CO}_2) = 44.63 \times 10^{-20} \text{ m}^2$ and $\sigma_{\text{geom}}(\text{N}_2) = 41.44 \times 10^{-20} \text{ m}^2$,³⁵ the much

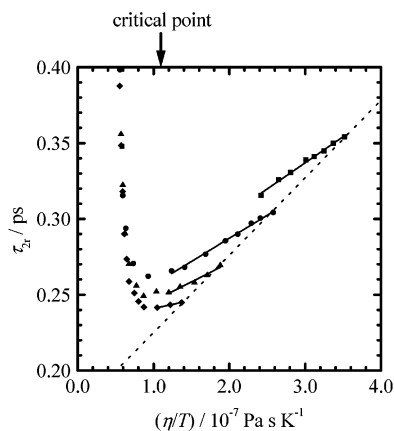


Figure 2. Relationship between τ_{2r} and η/T in CO_2 at 293.4 (■), 313.0 (●), 331.8 (▲), and 351.4 K (◆). The solid lines were obtained by linearly fitting the pressure-variable experimental data in the range of η/T more than $1.1 \times 10^{-7} \text{ Pa s K}^{-1}$, whereas the broken line was given by the linear regression of the temperature-variable experimental data at a fixed pressure of 20 MPa. The arrow represents the η/T value at the critical point.

larger difference in σ_{2r} between two molecules cannot be compensated enough. This fact strongly suggests that a large electric quadrupole moment of CO_2 can enhance the collision efficiency despite the similarity of nondipolar nature of two molecules. It has previously been reported as well that the collision cross sections of $\sigma_J(\text{CO}_2) = 59.9 \times 10^{-20} \text{ m}^2$ and $\sigma_J(\text{N}_2) = 14.9 \times 10^{-20} \text{ m}^2$ were determined from the angular momentum correlation times at 300 K.^{11,36} These observations are in harmony with the present results, whereas the ratio of $\sigma_J(\text{CO}_2)/\sigma_J(\text{N}_2)$ gives a relatively smaller value of ~ 4.0 .

In the liquidlike state, it was observed that $1/\tau_{2r}$ slightly decreases with increasing density. A molecular reorientation in a liquid phase has often been applied to the Debye diffusion model, and then related to a macroscopic viscosity, η , on the basis of the hydrodynamic model:

$$\tau_{2r} = a \times \frac{\eta}{T} + b \quad (5)$$

where T is the thermodynamic temperature. In the well-known Debye–Einstein–Stokes equation, $a = V/k_B$ and $b = 0$ with V being the volume of the spherical rotator. We attempt to plot τ_{2r} of CO_2 against η/T in Figure 2, where the η/T value at the critical point is shown by the arrow.³⁷ As is clearly seen from Figure 2, τ_{2r} linearly increases with a raise of η/T beyond the critical point's value of $\sim 1.1 \times 10^{-7} \text{ Pa s K}^{-1}$ at each temperature. The linear relationship between τ_{2r} and η/T at higher densities indicates that the molecular reorientation of CO_2 will be described by the Debye diffusion model, and again the nonlinear behavior of τ_{2r} at lower densities shows a failure of such a liquidlike model as discussed above. The slope a and intercept b were obtained by the least-squares fits of the data at fixed temperatures and also at a fixed pressure of 20 MPa (Table 3). It was found that the pressure-variable experiments at fixed temperatures give smaller a and larger b than the temperature-variable experiments at 20 MPa. Similar results have been observed in usual liquids or liquid solutions.^{38–40} In the pressure-variable experiments, moreover, a slightly decreases with increasing temperature, whereas b remains virtually constant of $\sim 0.23 \text{ ps}$. The negative temperature dependence of a suggests that the increase in a macroscopic viscosity can bring about the effective friction for the molecular reorientation of CO_2 ; however, its effect will be diminished as temperature, i.e., the

TABLE 3: Values of a and b in Eq 5 in the Plot of τ_{2r} vs η/T in CO_2 ^a

	293.4 K	313.0 K	331.8 K	351.4 K	20 MPa
$a/10^{-7} \text{ Pa}^{-1} \text{ K}$	3.44 (11)	3.06 (9)	2.52 (26)	1.09 (3)	5.11 (9)
b/ps	0.234 (3)	0.226 (2)	0.221 (4)	0.230 (1)	0.174 (2)

^a The 95% confidence limit in the least significant digits is given in parentheses. ^b Values of a and b were determined in the range of $\eta/T > \sim 1.1 \times 10^{-7} \text{ Pa s K}^{-1}$.

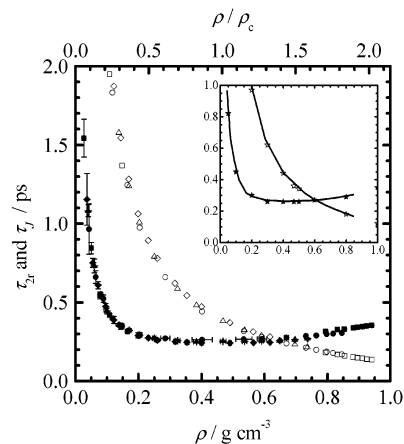


Figure 3. Density dependence of τ_{2r} (closed) and τ_J (open) of CO_2 at 293.4 (squares), 313.0 (circles), 331.8 (triangles), and 351.4 K (diamonds). In the inset, τ_{2r} (closed) and τ_J (open) of CO_2 calculated at 307 K by Adams and Siavosh-Haghighi²⁸ were shown by stars together with the solid lines between the experimental data (no symbols) at 313.0 K.

kinetic energy, increases. Recently, we have observed a similar temperature decrease in the slope a for the complex molecule in CO_2 .²⁴ On the other hand, the intercept b was sometimes interpreted as the free-rotor correlation time, $\tau_0 = (2\pi/9)(I/k_B T)^{0.5}$.^{41,42} Although τ_{2r} diverges infinitely at zero density limit, we can find that the extrapolated intercepts b are not far from the free-rotor correlation times, 0.27–0.29 ps, calculated in the present temperature range.

The reorientational correlation time τ_{2r} and the angular momentum correlation time τ_J of CO_2 are plotted against density in Figure 3, where we have reanalyzed the previous data^{9,10} of τ_J at different temperatures and densities (see Appendix). As shown in Figure 3, both τ_{2r} and τ_J steeply decrease with increasing density at lower densities, and only τ_{2r} moderately increases at higher densities. The temperature effect on the two correlation times is of little significance in the present temperature range except for τ_{2r} at higher densities. Figure 3 also indicates that the magnitude of τ_{2r} is smaller than that of τ_J at low densities, whereas $\tau_{2r} > \tau_J$ at high densities. The density at the crossing point is approximately 0.6 g cm^{-3} and slightly shifted to higher ones with increasing temperature. Although it was generally observed that τ_{2r} was much larger than τ_J in the usual liquids, τ_{2r} and τ_J in CO_2 are comparable to each other and differ only by a factor of ~ 2.6 even at liquidlike densities of $\rho > 0.6 \text{ g cm}^{-3}$. In the inset of Figure 3, we superpose τ_{2r} and τ_J recently calculated at 307 K by Adams and Siavosh-Haghighi²⁸ using molecular dynamics simulation. It was clearly demonstrated that the calculated correlation times are quite in a good agreement with the experimental correlation times over the entire observed range. This fact strongly suggests the reliability of τ_{2r} and the validity of the present experimental and analytical procedures.

There have been some dozen reports^{12–25} to examine the reorientational dynamics of solute molecules as a function of

solvent density in dilute binary supercritical solutions. In many cases^{14,16,19,22–25} τ_{2r} increased almost linearly with increasing macroscopic viscosity, and a remarkable increase in τ_{2r} at low densities as shown in this study was observed for a very few solute molecules.^{13,15,17,20} Hence, we hereafter have a brief discussion on the density dependence of reorientational dynamics in neat supercritical fluids. The experimental data of τ_{2r} has been available so far in C₂H₆,⁴³ SF₆,⁴⁴ CF₃H,⁴⁵ and D₂O³ over a wide density. Because intermolecular interactions should be the predominant factor in the density dependence of τ_{2r} , it is expected that a comparison of τ_{2r} between these fluids can provide meaningful information on the reorientational dynamics. A remarkable difference observed in the behaviors of τ_{2r} is the inversion density, at which τ_{2r} approaches to the minimum. In quadrupolar CO₂ the inversion was observed near the critical density. The inversion densities in dipolar CF₃H and strong hydrogen-bonding D₂O were less than the critical density, whereas those in nonpolar C₂H₆ and SF₆ were not so clear but appeared to be a little higher than the critical density. Thus, the inversion density increases in the order of D₂O \ll CF₃H \leq CO₂ \leq C₂H₆, SF₆. These observations seem to be very reasonable, and the reorientational dynamics of CO₂ reflects the nondipolar but quadrupolar nature strongly.

4. Conclusion

The precise measurements of ¹⁷O NMR longitudinal relaxation times, $T_1(^{17}\text{O})$, of CO₂ have been carried out under gaseous, liquid, and supercritical conditions. τ_{2r} values of CO₂ were determined from $T_1(^{17}\text{O})$ at four different temperatures of 293.4, 313.0, 331.8, and 351.4 K over a wide density range from 0.03 to 0.94 g cm⁻³. We have observed that τ_{2r} of CO₂ decreased rapidly with increasing density at lower densities and inversely increased at higher densities. It has clearly been demonstrated that the density dependence of τ_{2r} in CO₂ has a minimum near the critical density. The experimental τ_{2r} of CO₂ determined in the present study was quite in a good agreement with the calculated one by Adams and Siavosh-Haghighi²⁸ over the entire range. It has become apparent that τ_{2r} and τ_J are comparable even at liquidlike high densities in supercritical CO₂. Although the reorientational dynamics of CO₂ at higher densities will be semiquantitatively described by the Debye diffusion model, its time scale remains up to approximately subpicosecond, relatively shorter than conventional liquid solvents. The present results can provide a feasible picture of solvation dynamics of CO₂ around a solute or reaction species.

Appendix

¹³C longitudinal relaxation times, $T_1(^{13}\text{C})$, in CO₂ have previously been reported by Bai et al.⁹ in the range of 0.056 g cm⁻³ $< \rho < 0.95$ g cm⁻³ and 288.9 K $< T < 341.4$ K and by Etesse et al.¹⁰ in the range of 0.017 g cm⁻³ $< \rho < 1.09$ g cm⁻³ and 273 K $< T < 348$ K. τ_J of CO₂ was obtained from $T_1(^{13}\text{C})$ by substituting $C_\perp = 5.3 \times 2\pi$ kHz⁴⁶ and $I = 7.202 \times 10^{-46}$ kg m²⁴⁷ into eq 3. Because τ_J is considered to be the average time between collisions resulting in angular momentum energy transfers, the gas kinetic theory can give^{9–11,33}

$$\tau_J = \frac{1}{\rho_N \sigma_J \bar{v}} \quad (\text{A1})$$

Here, ρ_N is the number density, σ_J is the collision cross section, and \bar{v} is the mean relative velocity between collisional molecules. Moreover, it has been known that $\bar{v} \propto T^{1/2}$ and $\sigma_J \propto$

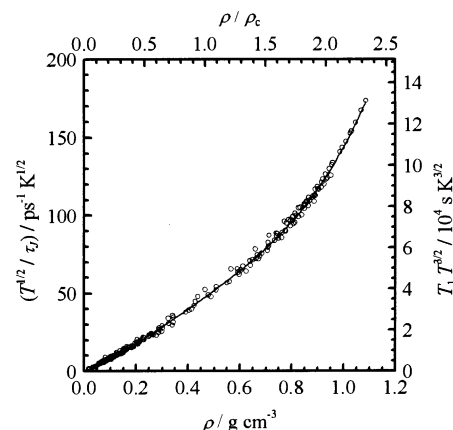


Figure 4. Plot of $T^{1/2}/\tau_J$ (left-hand axis) and $T_1 T^{3/2}$ (right-hand axis) vs density in CO₂. The solid line represents the biquadratic regression of the experimental data.

$T^{-1.10}$. Consequently, one can obtain

$$T^{1/2}/\tau_J \propto T_1 T^{3/2} \propto \rho \quad (\text{A2})$$

$T^{1/2}/\tau_J$ is plotted against CO₂ density in Figure 4. The density dependence of $T^{1/2}/\tau_J$ can be reproduced by the following polynomial equation within 14% errors over the entire range (please see the solid line in Figure 4):

$$T^{1/2}/\tau_J = a\rho + b\rho^2 + c\rho^3 + d\rho^4 \quad (\text{A3})$$

Here, the coefficients a , b , c , and d were $(68.3 \pm 3.1) \times 10^{12}$ cm³ K^{1/2} s⁻¹ g⁻¹, $(138.3 \pm 17.6) \times 10^{12}$ cm⁶ K^{1/2} s⁻¹ g⁻², $-(209.8 \pm 29.6) \times 10^{12}$ cm⁹ K^{1/2} s⁻¹ g⁻³, and $(147.0 \pm 15.2) \times 10^{12}$ cm¹² K^{1/2} s⁻¹ g⁻⁴, respectively. A τ_J value of CO₂ at a given density and temperature can be inter- or extrapolated according to eq A3.

Supporting Information Available: Additional experimental details; schematic drawing of high-pressure NMR cell (Figure S1), schematic diagram of high-pressure NMR setup (Figure S2), change in ¹⁷O signal of CO₂ in the inversion–recovery pulse sequence (Figure S3), and plot of the signal height against the variable delay time (Figure S4). This material is available free of charge via the Internet at <http://pubs.acs.org>.

References and Notes

- (1) Angus, S.; Armstrong, B.; de Reuck, K. M. *International Thermodynamic Table of the Fluid State-3 Carbon Dioxide*; IUPAC; Blackwell Science: Oxford, U.K., 1976.
- (2) See, for example: *Innovations in Supercritical Fluids*; Hutchenson, K. W.; Foster, N. R., Eds.; ACS Symposium Series, Volume 608; American Chemical Society: Washington, DC, 1995. *Chemical Synthesis Using Supercritical Fluids*; Jessop, P. G.; Leitner, W., Eds.; Wiley-VCH: New York, 1999.
- (3) Matubayasi, N.; Nakao, N.; Nakahara, M. *J. Chem. Phys.* **2001**, *114*, 4107.
- (4) Debye, P. *Polar Molecules*; Dover: New York, 1945.
- (5) *Spectroscopy and Relaxation of Molecular Liquids*; Steele, D., Yarwood, J., Eds.; Elsevier: Amsterdam, 1991. *Vibrational Spectra and Structure*; Durig, J. R., Ed.; Elsevier: Amsterdam, 1977; Vol. 6. Steele, W. A. *Adv. Chem. Phys.* **1977**, *34*, 1.
- (6) See, for example: Roy, M.; Doraiswamy, S. *J. Chem. Phys.* **1993**, *98*, 3213. Stratt, R. M.; Maroncelli, M. *J. Chem. Phys.* **1996**, *100*, 12981. Zhou, Y.; Constantine, S.; Harrel, S.; Gardecki, J. A.; Ziegler, L. D. *J. Raman Spectrosc.* **2000**, *31*, 85. Ernsting, N. P.; Photiadis, G. M.; Hennig, H.; Laurent, T. *J. Phys. Chem. A* **2002**, *106*, 9159.
- (7) See, for example: Hertz, H. G.; Zeidler, M. D. *Ber. Bunsen-Ges. Phys. Chem.* **1964**, *68*, 821. Jonas, J. *Acc. Chem. Res.* **1984**, *17*, 74. Grant, D. M.; Mayne, C. L.; Liu, F.; Xiang, T. *Chem. Rev.* **1991**, *91*, 1591. *Nuclear Magnetic Resonance Probes of Molecular Dynamics*; Tycko, R., Ed.; Kluwer Academic Press: Netherlands, 1994.

- (8) McConnell, J. *The Theory of Nuclear Magnetic Relaxation in Liquids*; Cambridge University: Cambridge, U.K., 1987.
- (9) Bai, S.; Mayne, C. L.; Pugmire, R. J.; Grant, D. M. *Magn. Reson. Chem.* **1996**, *34*, 479.
- (10) Etesse, P.; Zega, J. A.; Kobayashi, R. *J. Chem. Phys.* **1992**, *97*, 2022.
- (11) Jameson, C. J.; Jameson, A. K.; Smith, N. C.; Jackowski, K. *J. Chem. Phys.* **1987**, *86*, 2717.
- (12) Robert, J. M.; Evilia, R. F. *Anal. Chem.* **1988**, *60*, 2035.
- (13) Betts, T. A.; Zagrobelny, J.; Bright, F. V. *J. Am. Chem. Soc.* **1992**, *114*, 8163.
- (14) Howdle, S. M.; Bagratashvili, V. N. *Chem. Phys. Lett.* **1993**, *214*, 215.
- (15) Chen, S.; Miranda, D. T.; Evilia, R. F. *J. Supercrit. Fluids* **1995**, *8*, 255.
- (16) Anderton, R. M.; Kauffman, J. F. *J. Phys. Chem.* **1995**, *99*, 13759.
- (17) Heitz, M. P.; Bright, F. V. *J. Phys. Chem.* **1996**, *100*, 6889.
- (18) Bowman, L. E.; Palmer, B. J.; Garrett, B. C.; Fulton, J. L.; Yonker, C. R.; Pfund, D. M.; Wallen, S. L. *J. Phys. Chem.* **1996**, *100*, 18327.
- (19) Heitz, M. P.; Maroncelli, M. *J. Phys. Chem. A* **1997**, *101*, 5852.
- (20) deGrazia, J. L.; Randolph, T. W.; O'Brien, J. A. *J. Phys. Chem. A* **1998**, *102*, 1674.
- (21) Siavosh-Haghighi, A.; Adams, J. E. *J. Phys. Chem. A* **2001**, *105*, 2680.
- (22) Kauffman, J. F. *J. Phys. Chem. A* **2001**, *105*, 3433.
- (23) Patel, N.; Biswas, R.; Maroncelli, M. *J. Phys. Chem. B* **2002**, *106*, 7096.
- (24) Umecky, T.; Kanakubo, M.; Ikushima, Y. *J. Phys. Chem. B* **2002**, *106*, 11114.
- (25) Biswas, R.; Dahl, K.; Maroncelli, M. *J. Phys. Chem. B* **2002**, *106*, 11593.
- (26) Versmold, H. *Mol. Phys.* **1981**, *43*, 383.
- (27) Holz, M.; Haselmeier, R.; Dyson, A. J.; Huber, H. *Phys. Chem. Chem. Phys.* **2000**, *2*, 1717.
- (28) Adams, J. E.; Siavosh-Haghighi, A. *J. Phys. Chem. B* **2002**, *106*, 7973.
- (29) Kanakubo, M.; Aizawa, T.; Kawakami, T.; Sato, O.; Ikushima, Y.; Hatakeda, K.; Saito, N. *J. Phys. Chem. B* **2000**, *104*, 2749.
- (30) Umecky, T.; Kanakubo, M.; Ikushima, Y.; Saito, N.; Yoshimura, J.; Yamazaki, H.; Yana, J. *Chem. Lett.* **2002**, 118.
- (31) Wallen, S. C.; Schoenbachler, L. K.; Dawson, E. D.; Blatchford, M. A. *Anal. Chem.* **2000**, *72*, 4230.
- (32) Gripp, J.; Mäder, H.; Dreizler, H.; Teffo, J. L. *J. Mol. Spectrosc.* **1995**, *172*, 430.
- (33) Jameson, C. J. *Chem. Rev.* **1991**, *91*, 1375.
- (34) Jameson, C. J.; Jameson, A. K.; Horst, M. A. *J. Chem. Phys.* **1991**, *95*, 5799.
- (35) Maitland, G. C.; Rigby, M.; Smith, E. B.; Wakeham, W. A. *Intermolecular Forces, Their Origin and Determination*; Clarendon: London, 1981.
- (36) Jameson, C. J.; Jameson, A. K.; Smith, N. C. *J. Chem. Phys.* **1987**, *86*, 6833.
- (37) The viscosity of CO₂ was calculated according to the procedure of Altunin, V. V.; Sakhabetdinov, M. A. *Teploenergetika* **1972**, *8*, 85.
- (38) Jonas, J. *Annu. Rev. Phys. Chem.* **1975**, *26*, 167.
- (39) Ben-Amotz, D.; Jeanloz, R.; Harris, C. B. *J. Chem. Phys.* **1987**, *86*, 6119.
- (40) Wakai, C.; Nakahara, M. *J. Chem. Phys.* **1995**, *103*, 2025.
- (41) Bai, S.; Taylor, C. M. V.; Liu, F.; Mayne, C. L.; Pugmire, R. J.; Grant, D. M. *J. Phys. Chem. B* **1997**, *101*, 2923.
- (42) Yonker, C. R. *J. Phys. Chem. A* **2000**, *104*, 685.
- (43) Baglin, F. G.; Versmold, H.; Zimmermann, U. *Mol. Phys.* **1984**, *53*, 1225.
- (44) Zerda, T. W.; Schroeder, J.; Jonas, J. *J. Chem. Phys.* **1981**, *75*, 1612.
- (45) Okazaki, S.; Matsumoto, M.; Okada, I. *J. Chem. Phys.* **1995**, *103*, 8594.
- (46) Amos, R. D.; Battaglia, M. R. *Mol. Phys.* **1978**, *36*, 1517.
- (47) Chan, F. T.; Tang, C. L. *J. Appl. Phys.* **1969**, *40*, 2806.